Comparison of Monte Carlo and anharmonic-lattice-dynamics results for the thermodynamic properties and atomic mean-square displacement of Xe using the Morse potential

R. C. Shukla, S. K. Bose, and R. F. Delogu
Physics Department, Brock University, St. Catharines, Ontario, Canada L2S 3A1
(Received 9 September 1991)

Monte Carlo (MC) and anharmonic-lattice-dynamics [the λ^2 and λ^4 perturbation-theory (PT)] calculations of the thermodynamic properties of Xe are presented for the temperature range 60–160 K using a nearest-neighbor central-force (NNCF) model of the fcc crystal with atoms interacting via a Morse potential. In particular, we calculate the equilibrium lattice parameter at zero pressure and the corresponding specific heats at constant volume and at constant pressure, volume expansivity, adiabatic and isothermal bulk moduli, and Grüneisen parameter. We also calculate the atomic mean-square displacement (MSD) from the MC method and the lowest-order (λ^2) PT for the same NNCF model and the Morse potential. For the thermodynamic properties, the MC results are found to agree more closely with the λ^2 PT than the λ^4 PT results. Similarly the MSD results from the MC method agree quite well with those from the λ^2 theory. This may be due to the fact that the exact solution of the Schrödinger equation for the vibrational states of the Morse potential for a one-dimensional or an isotropic three-dimensional model agrees exactly with the λ^2 PT. We show that this is indeed true by evaluating the λ^2 and λ^4 contributions to vibrational energy for the above model of the Morse potential and showing that all the λ^4 contributions add up to zero and that the total λ^2 contribution is in agreement with the solution of the Schrödinger equation.

I. INTRODUCTION

The purpose of this work is to report some results for the thermodynamic properties for solid Xe from our Monte Carlo (MC) calculations and the anharmonic perturbation theory. The model for solid xenon, used in these calculations, remains the same as in the earlier calculation,[1] viz., a nearest-neighbor central-force (NNCF) model of the fcc lattice where the atoms are interacting pairwise via a Morse potential. The motivation for this work comes from the fact that extensive numerical results exist in the literature[1] for the various thermodynamic properties for this model and this potential from the quasiharmonic (QH) theory, the lowest-order anharmonic (cubic and quartic), λ^2, perturbation theory (PT), and the next-higher-order, λ^4, anharmonic perturbation theory. Since no Taylor's expansion of the crystal potential energy is involved in the MC method and thereby *all* anharmonic contributions are contained in its numerical results for the various thermodynamic properties, the MC results can be very useful in comparing these with those of the λ^2 and λ^4 perturbation theories. In an earlier publication[1] by one of us, the thermodynamic results for solid Xe from the λ^2 and λ^4 perturbation theories for the NNCF model and Morse potential were compared with the real experimental data. Once the MC results are available, they can be compared with the λ^2 and λ^4 PT results. For a given potential function this would be a more meaningful comparison because a real solid may not be represented by either a Morse potential or the most widely used 6-12 Lennard-Jones potential. For an LJ solid extensive comparisons of the results of the above theories and the MC method have been made by Shukla and Cowley[2] and Heiser, Shukla, and Cowley[3] for the thermodynamic properties and average square atomic displacement, respectively. In comparing the MC results with the λ^4 perturbation theory, Shukla and Cowley found the best agreement with a subset of four diagrams of $O(\lambda^4)$ for the LJ case. This subset was identified as the ISC (improved self-consistent) set because to $O(\lambda^4)$ these are the only diagrams contained in the ISC scheme of Goldman, Horton, and Klein.[4] In this paper we will make comparisons of the numerical magnitudes of all the λ^4 diagrams for the LJ and Morse potentials along with the subtotals of the λ^4 set. It will be apparent from this comparison that for the Morse potential the results for the λ^2 PT and ISC scheme are essentially the same due to a heavy cancellation of the diagrams in the ISC set.

To facilitate our presentation and discussion of the results of the λ^2 and λ^4 perturbation theories, we present in Sec. II a summary of these theories. Monte Carlo calculations are summarized in Sec. III and the results of these calculations are compared and discussed in Sec. IV. The conclusion of this work is given in Sec. V.

II. PERTURBATION THEORIES OF ORDER λ^2 AND λ^4

When perturbation theory (PT) is employed in the calculation of the Helmholtz function (F) of an anharmonic crystal, the various anharmonic contributions to F are obtained in the form of an infinite series. This is so because the perturbing potential is itself in the form of an infinite series. Thus in the systematic application of PT

in the calculation of F, whose minimization gives the thermodynamic properties, one needs to know the number of terms to be retained in a given order of PT.

The Hamiltonian needed for the enumeration of the various contributions to F to order λ^2 and λ^4, respectively, is given by

$$H = H_0 + \lambda V_3 + \lambda^2 V_4 + \lambda^3 V_5 + \lambda^4 V_6 = H_0 + V \ , \quad (1)$$

where H_0 is the harmonic portion of H; λ is the Van Hove perturbation expansion parameter, which is defined as the ratio of a typical root-mean-square displacement and the nearest-neighbor distance, and V_3 to V_6 are the cubic, quartic, etc., terms in the Taylor's expansion of the crystal potential energy. With the above H, F is evaluated from $F = -(1/\beta)\ln Z$, where $Z = \mathrm{Tr} e^{-\beta H}$, $\beta = 1/k_B T$, and Tr represents the trace of the operator $\exp(-\beta H)$. Since the operators H_0 and V in the above H do not commute with each other, the expansion of $e^{-\beta H}$ can be carried out in the form of $e^{-\beta H_0} S(\beta)$, where $S(\beta)$ is an infinite series involving various powers of V, the total perturbing potential in Eq. (1). These terms can be evaluated by the diagrammatic method. When the diagrammatic method is employed in the evaluation of F, the contributions can be grouped according to the powers of λ. For example, one finds *two* contributions of $O(\lambda^2)$ and *eight* contributions of $O(\lambda^4)$ for a centrosymmetric crystal. Extensive details of this diagrammatic procedure have been presented by Shukla and Cowley.[5] The diagrams of $O(\lambda^2)$ and $O(\lambda^4)$ are presented in this paper in Figs. 1 and 2, respectively, for the purposes of describing the calculations and discussion of the various results.

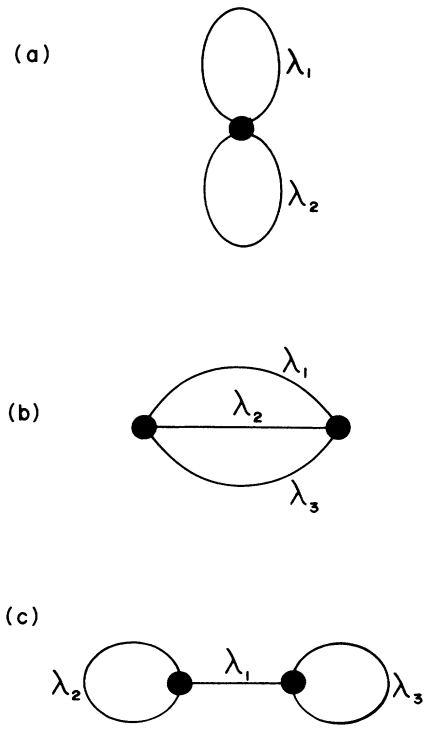

FIG. 1. Diagrams of order λ^2.

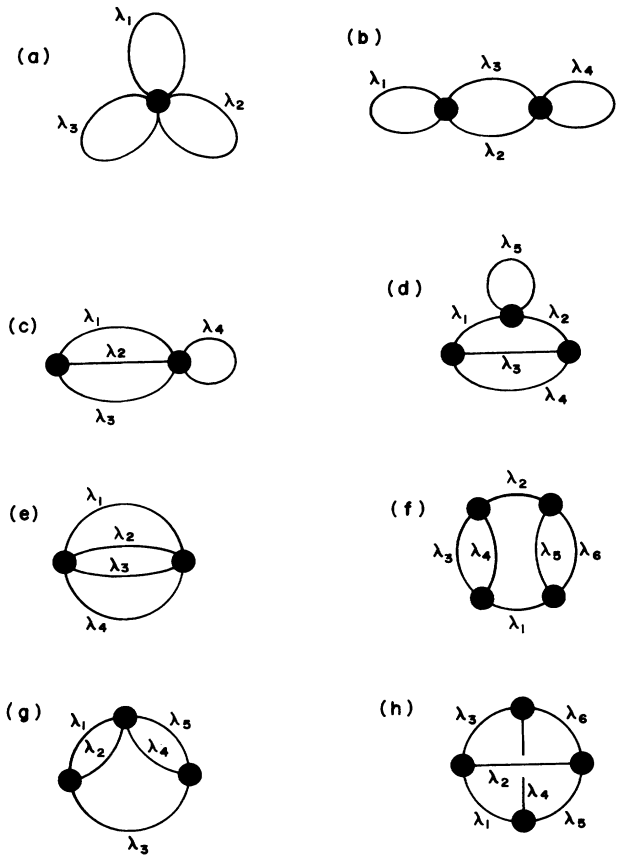

FIG. 2. Diagrams of order λ^4.

The solid dots represent the anharmonic vertices, and lines connecting them are phonon propagators. The labels λ_i $(i = 1,2,3,\ldots,n)$ collectively represent the wave vectors $\mathbf{q}_i$ and branch indices j_i. Since diagram 1(c) in Fig. 1 gives zero contribution for all Bravais lattices and/or lattices with a basis provided that each atom is at a center of inversion symmetry, we have omitted *all* diagrams of this type from Fig. 2.

Although these diagrams are of order λ^2 and λ^4, which erroneously might imply the use of only the second and fourth order of PT, they arise in different orders of PT. For example, the two diagrams of $O(\lambda^2)$ presented in Fig. 1, viz., 1(a) and 1(b), arise in the first and second orders of PT, respectively, whereas the eight diagrams of $O(\lambda^4)$ presented in Fig. 2 arise in PT of different orders, i.e., 2(a) arises in the first, order, 2(b), 2(c), and 2(e) in the second order, 2(d) and 2(g) in the third order, and finally 2(f) and 2(h) in the fourth order. But according to the Van Hove ordering scheme, all these eight diagrams are of order λ^4.

Having presented the details of the calculations in previous papers, it will suffice here to summarize the necessary equations for the calculations of the equation of state to $O(\lambda^2)$. To this order the minimum of the free energy with respect to volume (V) is obtained from

$$F = U + F_{\mathrm{QH}} + F_{1a} + F_{1b} \ , \quad (2)$$

where U is the static energy which is obtained by sum-

ming the Morse potential (ϕ_m) over the nearest neighbors. ϕ_m with its functional form and parameters for Xe is given in Sec. III. Expressions for $F_{\rm QH}$ (the quasiharmonic contribution to F), F_{1a}, and F_{1b} (the λ^2 contributions to F) in the high-temperature limit ($T > \Theta_D$, Θ_D is the Debye temperature) are taken from Shukla[6] and Shukla and MacDonald.[7] These expressions are

$$F_{\rm QH}=3Nk_BT\left\{\ln\left[\frac{\hbar^2}{k_BT}\left[\frac{8}{M}\sqrt{B}\right]\right]-0.428\,834\,8+0.5f(a_1)\right\}+3N\left[\frac{1}{6}\frac{\hbar^2}{M}\frac{1}{k_BT}\right]B(1+3a_1)\,, \tag{3}$$

$$F_{1a}=\frac{N(k_BT)^2}{64B^2}\left[DS_{4A}(a_1)+\frac{2C}{r}S_{4B}(a_1)+\frac{4B}{r^2}S_{4C}(a_1)\right]\,, \tag{4}$$

$$F_{1b}=-\frac{N(k_BT)^2}{3072B^3}\left[C^2S_{3A}(a_1)+\frac{12BC}{r}S_{3B}(a_1)+\frac{4B^2}{r^2}S_{3C}(a_1)\right]\,, \tag{5}$$

where $\hbar$ is the Planck's constant divided by 2π, M is the atomic mass, k_B is the Boltzmann constant, T is the temperature, and N represents the number of unit cells in the crystal. B,C,D are the various combinations of the derivatives of the two-body potential $\phi(r)$. They are defined in terms of the operator $O=(1/r)d/dr$ as $B=r^2O^2\phi(r)$, $C=r^3O^3\phi(r)$, and $D=r^4O^4\phi(r)$. $f(a_1)$ is the Brillouin-zone (BZ) sum in the quasiharmonic free energy. Similarly, S_{3A}, etc., in F_{1b} and S_{4A}, etc. in F_{1a} are the various BZ sums which are computed as a function of the parameter $a_1=\phi'/(r\phi''-\phi')$. This parameter characterizes the volume dependence of these BZ sums. In Shukla and MacDonald the calculated values[6] for each of these sums, in the interval $-0.1\le a_1\le 0.1$, have been fitted to an exponential of a polynomial function of sixth degree. The coefficients of this polynomial are given in their paper. The λ^4 contributions to F have been evaluated by the same procedure as presented in Shukla and Wilk[8] and Shukla and Cowley[2] in their calculations for the LJ potential. We have followed the same procedure for the Morse potential. In the calculation of equation of state the total energy given by Eq. (2) is minimized to get the zero-pressure volume or the nearest-neighbor distance r for a given T. The subsequent calculation of C_p, C_v, etc. requires the evaluation of B,C,D at this value of r.

The mean-square displacement to $O(\lambda^2)$ has been calculated from the following high-temperature-limit quasiharmonic and the $O(\lambda^2)$ (cubic and quartic) expressions:[3]

$$\langle u^2\rangle_{\rm QH}=\frac{k_BT}{NM}\sum_{\mathbf{q},j}\frac{1}{\omega_{\mathbf{q}j}^2}\,, \tag{6}$$

$$\langle u^2\rangle_{Q}=-\frac{(k_BT)^2\lambda^2}{2N^2M}\sum_{\mathbf{q}_1,j_1}\sum_{\mathbf{q}_2,j_2}\frac{\Phi(\mathbf{q}_1,j_1;-\mathbf{q}_1,j_1;\mathbf{q}_2,j_2;-\mathbf{q}_2,j_2)}{\omega_{\mathbf{q}_1j_1}^2\omega_{\mathbf{q}_2j_2}^4}\,, \tag{7}$$

$$\langle u^2\rangle_{C}=\frac{(k_BT)^2\lambda^2}{2N^2M}\sum_{\substack{\mathbf{q}_1,\mathbf{q}_2,\mathbf{q}_3\\ j_1,j_2,j_3}}\Delta(\mathbf{q}_1+\mathbf{q}_2+\mathbf{q}_3)\frac{|\Phi(\mathbf{q}_1,j_1;\mathbf{q}_2,j_2;\mathbf{q}_3,j_3)|^2}{\omega_{\mathbf{q}_1j_1}^2\omega_{\mathbf{q}_2j_2}^2\omega_{\mathbf{q}_3j_3}^4}\,. \tag{8}$$

The various symbols appearing in Eqs. (6)–(8) have the following meaning: The Δ function $\Delta(\mathbf{q}_1+\mathbf{q}_2+\cdots+\mathbf{q}_n)$ appearing in Eq. (8) is unity if $(\mathbf{q}_1+\mathbf{q}_2+\cdots+\mathbf{q}_n)$ is zero or a vector of the reciprocal lattice (τ) and zero otherwise. The Φ functions appearing in Eqs. (7) and (8) are the Fourier transforms of the fourth- and third-order atomic force constants, respectively, which in the present calculation are obtained from $\phi(r)$. In general, the Fourier transform of the nth-order tensor atomic force constant $\phi_{\alpha\beta}\cdots\mu(l)$ is defined by the following:

$$\Phi(\mathbf{q}_1j_1,\mathbf{q}_2j_2,\ldots,\mathbf{q}_nj_n)=\frac{1}{2M^{n/2}}\sum_{l}{}'\sum_{\alpha,\beta,\ldots,\mu}\phi_{\alpha\beta\cdots\mu}(l)\epsilon_\alpha(\mathbf{q}_1j_1)\cdots\epsilon_\mu(\mathbf{q}_nj_n)\times(1-e^{i\mathbf{q}_1\cdot\mathbf{r}_l})(1-e^{i\mathbf{q}_2\cdot\mathbf{r}_l})\cdots(1-e^{i\mathbf{q}_n\cdot\mathbf{r}_l})\,,$$

where the prime over the direct lattice vector (l) summation in the previous equation indicates the omission of the origin point. $\omega(\mathbf{q}j)$ and $\epsilon(\mathbf{q}j)$ are the eigenvalues and eigenvectors, respectively, for the wave vector $\mathbf{q}$ and branch index j. These are calculated for the nearest-neighbor model of the fcc lattice for the Morse potential.

For comparison with MC results, where all calculations have been done with 256 particles, we have calculat-

ed the MSD from Eqs. (6)–(8) for 256 wave vectors by omitting the origin from the normalization procedure. We have also calculated the best converged values for MSD from the method recently proposed by Shukla and Plint[9] for the calculation of the Debye-Waller factor or MSD for fcc systems.

III. MONTE CARLO SIMULATION

Monte Carlo simulation of solid Xe was carried out using the Metropolis scheme[10] for a set of six temperatures on an equispaced grid between 60 and 160 K. The potential energy U of the solid was written as a sum of pair potentials ϕ:

$$U=\tfrac{1}{2}\sum_{i\neq j}\phi(r_{ij}) \tag{9}$$

and ϕ was chosen to be the Morse potential, ϕ_m:

$$\phi_m(r)=\epsilon(e^{-2\alpha(r-r_0)}-2e^{-\alpha(r-r_0)}) , \tag{10}$$

with the parameters ϵ, α, and r_0 determined by fitting[1] to the zero-temperature experimental values of the sublimation energy, lattice constant, and bulk modulus ($\epsilon=4.576\times10^{-14}$ erg, $r_0=4.321$ Å, $\alpha=1.375$ Å^{-1}) including the zero-point energy. The pressure P was determined from the canonical ensemble average (denoted by angular brackets) of the pressure function, π (Refs. 11–13):

$$P=\langle\pi\rangle=\left\langle\frac{N}{V}k_BT-\frac{1}{3V}\sum_{1\le i\le j}^{N}r_{ij}\frac{\partial\phi}{\partial r_{ij}}\right\rangle , \tag{11}$$

where N is the number of particles in the system, V is its volume, and k_B is the Boltzmann constant. The specific heat at constant volume, C_v in units of the universal gas constant R, was calculated from the fluctuations in the potential energy using[10–13]

$$C_v=\tfrac{3}{2}+\langle(\delta U)^2\rangle/N(k_BT)^2 , \tag{12}$$

where $\delta U=U-\langle U\rangle$.

The specific heat at constant pressure, C_p, was determined using the relation

$$C_p-C_v=-T\left[\frac{\partial P}{\partial T}\right]_V^2\Big/\left[\frac{\partial P}{\partial V}\right]_T . \tag{13}$$

$(\partial P/\partial T)_V$ was calculated from the canonical ensemble average of the fluctuations in the potential energy and the pressure function:[11–13]

$$\left[\frac{\partial P}{\partial T}\right]_V=\frac{N}{V}k_B+\langle(\delta U\delta\pi)\rangle/k_BT^2 , \tag{14}$$

where $\delta\pi=\pi-\langle\pi\rangle$.

$(\partial P/\partial V)_T$ was determined graphically for each temperature. Isothermal (B_T) and adiabatic (B_S) bulk modulii, volume expansitivity (β), and the Grüneisen parameter (γ) were calculated from

$$B_T=-V\left[\frac{\partial P}{\partial V}\right]_T , \tag{15}$$

$$B_S=(C_p/C_v)B_T , \tag{16}$$

$$\beta=\frac{1}{V}\left[\frac{\partial V}{\partial T}\right]_P \tag{17}$$

$$=-\frac{1}{V}\left[\frac{\partial P}{\partial T}\right]_V\Big/\left[\frac{\partial P}{\partial V}\right]_T , \tag{18}$$

$$\gamma=\frac{\beta VB_T}{C_v} . \tag{19}$$

Simulation was performed on 256 particles using periodic-boundary conditions and the starting configuration for each temperature was chosen to be fcc. Random numbers distributed uniformly in the range [0,1] were used to determine the magnitude of the displacement in each trial. The maximum allowed displacement in a given trial was chosen to keep the fraction of successful moves around 50% for simulations between 60 and 100 K. For higher temperatures, ~(120–160 K), a smaller maximum displacement (hence a higher success rate, ~60%) was allowed to prevent jumps that would necessitate updating the list of nearest neighbors. Potential energy was calculated using the Morse potential given by Eq. (10) for the nearest neighbors and the interaction between further neighbors was set to zero. For all temperatures the simulation was carried out for a fixed list of nearest neighbors. For temperatures between 60 and 100 K, the initial $\sim7\times10^5$ configurations were discarded from the calculation of the averages as the system would equilibriate during this time. Canonical averages were computed from the next $\sim1.2\times10^6$ configurations with the usual accountancy rule that an unchanged configuration, after a move is rejected, should be counted as a new configuration. For temperatures between 120–160 K, where a small step size (maximum allowed displacement) was used, a larger number of configurations, $\sim2\times10^6$, was used both for establishing the equilibrium and the calculation of the averages.

For each temperature the volume of the system, or equivalently the lattice parameter, was varied until the calculated pressure was zero to within a few parts in 10^3. Thermodynamic quantities were then computed for this lattice parameter. The quantity $(\partial P/\partial V)_T$ was estimated graphically from a few pairs of pressure and volume around the zero-pressure value. The quantities directly computed from the simulation were the equilibrium (zero-pressure) lattice constants, C_v [via Eq. (12)]; $(\partial P/\partial T)_V$ [via Eq. (14)], $(\partial P/\partial V)_T$ (determined graphically); and the rest followed from Eqs. (13) and (15)–(19). The values of the thermodynamic quantities computed from the simulation had converged within 1–2%.

For each of the above temperatures we have also calculated the mean-square displacements of the atoms in the 256-particle cluster. Displacements of the particles from their corresponding crystalline positions (fcc lattice with lattice parameter appropriate to the given temperature) were considered. During the simulation the cluster drifts through space. No attempt was made to hold the center

of mass of the cluster fixed and particle coordinates were always expressed relative to the corresponding center-of-mass position. After a complete cycle, in which each particle in the cluster was attempted to move once, the center of mass for the cluster was calculated. The particle coordinates were expressed relative to the current center-of-mass positions, and the average of the square of the displacements of the 256 atoms from their corresponding crystalline positions (expressed relative to the center of mass of the initial rigid lattice) was computed. The final average was computed by considering averages over the cycles and the simulation was continued till the calculated root-mean-square displacements had converged to within 0.1%. Results of the 256-particle cluster Monte Carlo simulations for the mean-square displacements are compared with the lattice-dynamics results in Table II.

IV. RESULTS AND DISCUSSION

The results for the various thermodynamic properties of Xe from the quasiharmonic (QH), λ^2 and λ^4, and MC method are presented in Figs. 3–9. The experimental values (represented by dots) are taken from Korpium and Lüscher.[14] It is clear from these results that overall the

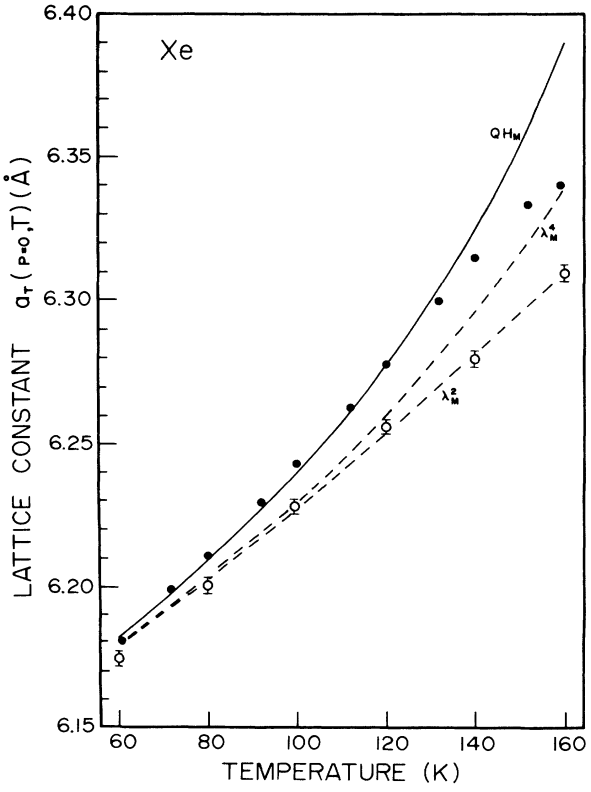

FIG. 3. Lattice constant (a_T) at zero pressure for Xe. Dots, experimental data; dashed lines, nearest-neighbor Morse potential. QH denotes quasiharmonic results; similarly, λ^2 and λ^4 denote perturbation-theory results to $O(\lambda^2)$ and $O(\lambda^4)$, respectively. Big open circles denote the Monte Carlo results.

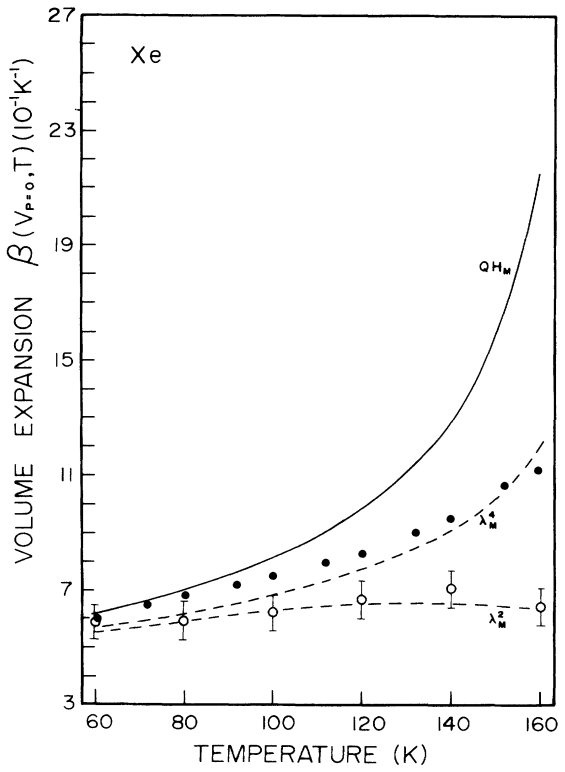

FIG. 4. Volume expansion (β) for Xe. Points and lines have the same meaning as in Fig. 3.

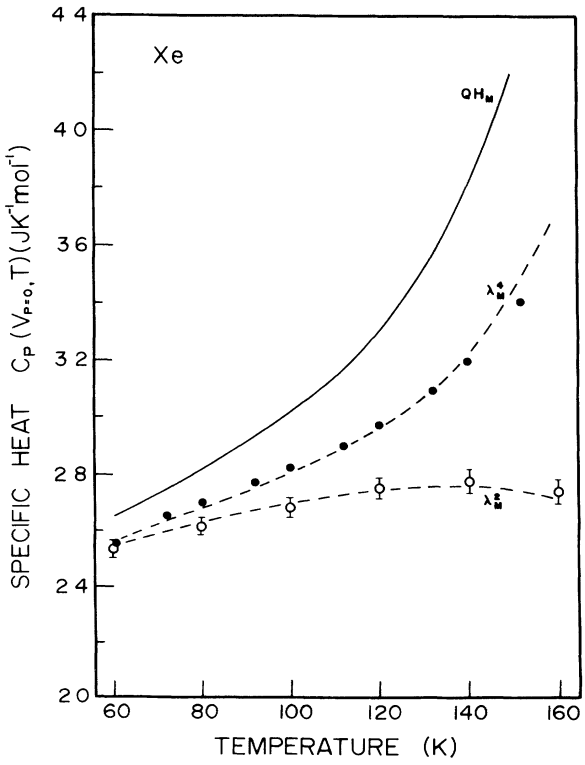

FIG. 5. Specific heat at constant volume (C_v). Points and lines have the same meaning as in Fig. 3.

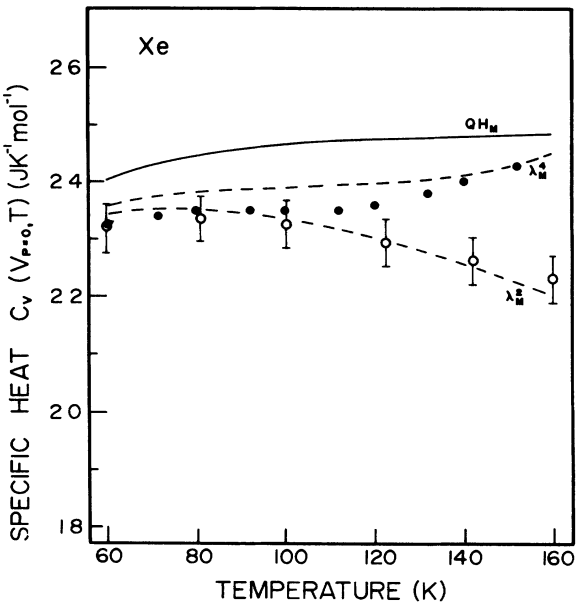

FIG. 6. Specific heat at constant pressure (C_p) for Xe. Points and lines have the same meaning as in Fig. 3.

QH results for the Morse potential do not come out that badly for most of the thermodynamic properties and the best overall agreement with experiment is achieved with the λ^4 theory. However, the MC results for almost all of the thermodynamic properties agree much more closely

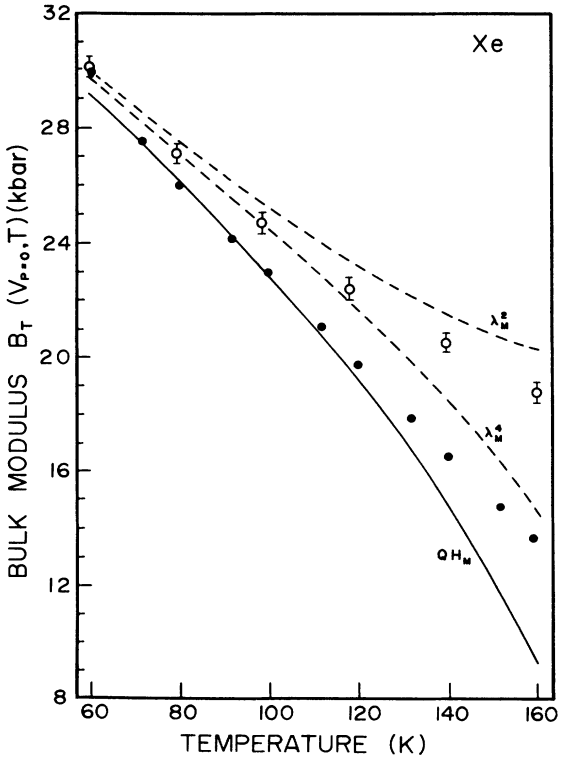

FIG. 7. Isothermal bulk modulus (B_T) for Xe. Points and lines have the same meaning as in Fig. 3.

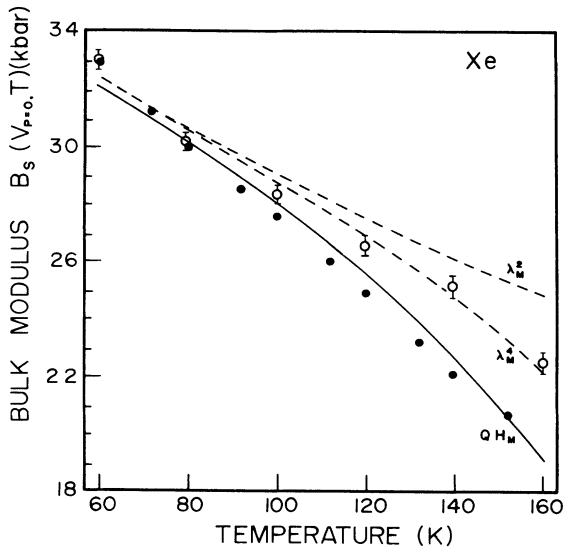

FIG. 8. Adiabatic bulk modulus (B_S) for Xe. Points and lines have the same meaning as in Fig. 3.

with the λ^2 theory than the λ^4 theory. Both the λ^2 and MC results disagree with the experimental data points. This is somewhat surprising in view of the fact that *all* anharmonic contributions are contained in the MC results. A possible explanation of this is needed, which we provide here for a one-dimensional or a three-dimensional isotropic system. It is a well-known fact that for such a system there exists an exact solution of the Schrödinger equation for the vibrational energy states.[15] For a quantum state n the energy levels for the Morse potential are given by

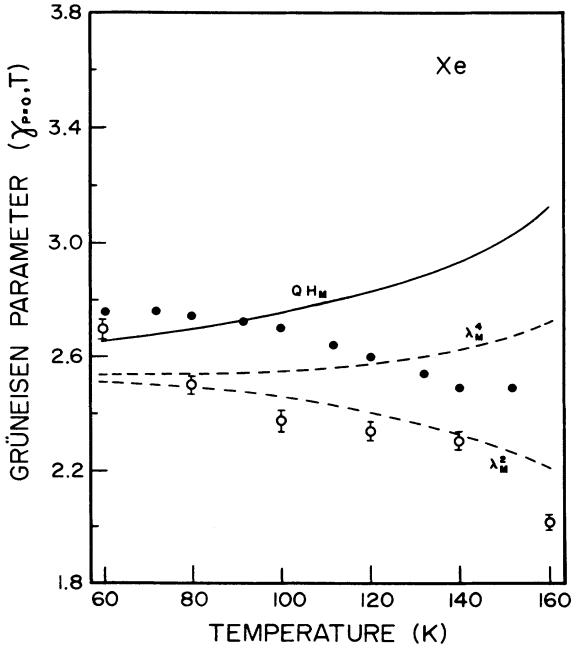

FIG. 9. Grüneisen parameter (γ) for Xe. Points and lines have the same meaning as in Fig. 3.

$$E_n=\hbar\omega(n+\tfrac{1}{2})-\hbar\omega x(n+\tfrac{1}{2})^2 , \tag{20}$$

where ω is the harmonic frequency of the oscillator and ωx is the anharmonic frequency.

How well does this compare with the results of PT to orders λ^2, λ^4, etc? The answer is that it agrees exactly to $O(\lambda^2)$ because the next order λ^4 contribution to E_n is identically zero. To demonstrate this, we consider the following Hamiltonian in terms of creation ($a^\dagger$) and annihilation (a) operators,

$$H=\hbar\omega(a^\dagger a+\tfrac{1}{2})+\sum_{n=3}^{6}\lambda^{n-2}K_n\left[\frac{\hbar}{2m\omega}\right]^{n/2}(a^\dagger+a)^n , \tag{21}$$

where λ is the Van Hove perturbation expansion parameter, $K_n=\phi^n(r)/n!$ and $\phi^n(r)$ represents the nth derivative of $\phi(r)$. In an obvious notation, if we write the above H as

$$H=H_0+\lambda H_3+\lambda^2H_4+\lambda^3H_5+\lambda^4H_6 , \tag{22}$$

the energy formula for the nth state of the oscillator to $O(\lambda^4)$ can be derived from the time-independent perturbation theory. Denoting the λ^2 and λ^4 contributions by $E_n(\lambda^2)$ and $E_n(\lambda^4)$, respectively, we get

$$E_n(\lambda^2)=\langle n|H_4|n\rangle+\sum_{k\neq n}\frac{\langle n|H_3|k\rangle\langle k|H_3|n\rangle}{(E_0^n-E_0^k)} , \tag{23}$$

$$\begin{aligned}E_n(\lambda^4)=&\langle n|H_6|n\rangle+\sum_{l\neq n}\frac{\langle n|H_4|l\rangle\langle l|H_4|n\rangle}{(E_0^n-E_0^l)}+2\sum_{m\neq n}\frac{\langle n|H_5|m\rangle\langle m|H_3|n\rangle}{(E_0^n-E_0^m)}\\&+\sum_{j(j\neq n)}\sum_{m(m\neq n)}\frac{\langle n|H_3|j\rangle\langle j|H_4|m\rangle\langle m|H_3|n\rangle}{(E_0^n-E_0^j)(E_0^n-E_0^m)}+\sum_{l\neq n}\sum_{j\neq n}\frac{\langle n|H_3|j\rangle\langle j|H_3|l\rangle\langle l|H_4|n\rangle}{(E_0^n-E_0^j)(E_0^n-E_0^l)}\\&+\sum_{l\neq n}\sum_{m\neq n}\frac{\langle n|H_4|l\rangle\langle l|H_3|m\rangle\langle m|H_3|n\rangle}{(E_0^n-E_0^l)(E_0^n-E_0^m)}\\&+\sum_{j(j\neq n)}\sum_{l(l\neq n)}\sum_{m(m\neq n)}\frac{\langle n|H_3|j\rangle\langle j|H_3|l\rangle\langle l|H_3|m\rangle\langle m|H_3|n\rangle}{(E_0^n-E_0^j)(E_0^n-E_0^l)(E_0^n-E_0^m)}-E_n(\lambda^2)\sum_{p\neq n}\frac{\langle n|H_3|p\rangle\langle p|H_3|n\rangle}{(E_0^n-E_0^p)^2} ,\end{aligned} \tag{24}$$

where E_0^n or others with different superscripts are the energy states of the harmonic oscillator. A straightforward but tedious calculation of the matrix elements in the above two equations gives the following results for $E_n(\lambda^2)$ and $E_n(\lambda^4)$:

$$E_n(\lambda^2)=K_4\left[\frac{\hbar}{2m\omega}\right]^2(6n^2+6n+3)-K_3^2\left[\frac{\hbar}{2m\omega}\right]^3\left[\frac{1}{\hbar\omega}\right](30n^2+30n+11) , \tag{25}$$

$$\begin{aligned}E_n(\lambda^4)=&K_6\left[\frac{\hbar}{2m\omega}\right]^3(20n^3+30n^2+40n+15)-K_4^2\left[\frac{\hbar}{2m\omega}\right]^4\left[\frac{1}{\hbar\omega}\right](68n^3+102n^2+118n+42)\\&-K_3K_5\left[\frac{\hbar}{2m\omega}\right]^4\left[\frac{1}{\hbar\omega}\right](280n^3+420n^2+400n+130)\\&+K_3^2K_4\left[\frac{\hbar}{2m\omega}\right]^5\left[\frac{1}{\hbar\omega}\right]^2(1800n^3+2700n^2+2268n+684)\\&-K_3^4\left[\frac{\hbar}{2m\omega}\right]^6\left[\frac{1}{\hbar\omega}\right]^3(2820n^3+4230n^2+3270n+930) .\end{aligned} \tag{26}$$

Now at this point in the calculation if we substitute $m\omega^2=\phi''(r_0)$, $K_4=\phi^{iv}(r_0)/4!$, and $K_3=\phi'''(r_0)/3!$ into Eq. (25), $E_n(\lambda^2)$ can be written as

$$E_n(\lambda^2)=\frac{\phi^{iv}(r_0)\hbar^2\omega^2}{16[\phi''(r_0)]^2}(n^2+n+\tfrac{1}{2})-\frac{[\phi'''(r_0)]^2\hbar^2\omega^2}{96[\phi''(r_0)]^2}(10n^2+10n+\tfrac{11}{3}) ,$$

where for the Morse potential, $\phi''(r_0)=2\alpha^2\epsilon$, $\phi'''(r_0)=-6\alpha^3\epsilon$, $\phi^{iv}(r_0)=14\alpha^4\epsilon$. Substituting these derivatives in the above equation, we get

$$E_n(\lambda^2)=-(n+\tfrac{1}{2})^2\left[\frac{\hbar^2\omega^2}{4\epsilon}\right] ,$$

which when combined with the zero-order solution of the harmonic Hamiltonian H_0, viz., $(n+\frac{1}{2})\hbar\omega$, gives the

TABLE I. Contributions to the free energy of $O(\lambda^4)$ for the LJ and Morse potentials in units of $N(k_BT)^3/\epsilon^2$.

Diagram	Contribution LJ	Partial total LJ	Contribution Morse	Partial total Morse
2(a)	0.2048		0.0517	
2(b)	−0.6423	F(SC1)=−0.4375	−0.2385	F(SC1)=−0.1867
2(c)	−0.6000		−0.2371	
2(d)	0.9403	F(ISC)=−0.0972	0.4203	F(ISC)=−0.0035
2(e)	−0.2231		−0.1071	
2(f)	−0.3548	F(SC2)=−0.6751	−0.1938	F(SC2)=−0.3045
2(g)	0.5946		0.2964	
2(h)	−0.0929	$F(\lambda^4)$=−0.1733	−0.0497	$F(\lambda^4)$=−0.0579

same energy as given by Eq. (20). Turning our attention now to $E_n(\lambda^4)$, as given by Eq. (26), all that is required is to substitute for the derivatives K_3 to K_6 for the Morse potential evaluated at $r=r_0$ and calculate the total coefficient for each of the n^3, n^2, n, and the constant term. We omit the algebra and simply state that each of these terms is identically zero. Thus we find that at least to $O(\lambda^4)$ of perturbation theory the PT result agrees with the exact solution. However, it should be noted that if the derivatives are evaluated at any value other than $r=r_0$, there will be a small correction from $E_n(\lambda^4)$. This may be the reason why the PT results for the thermodynamic properties to $O(\lambda^2)$ and $O(\lambda^4)$ differ from each other. Based on the above arguments and the fact that the MC results have come out almost the same as the λ^2 PT results, it is safe to conclude that if there is some way to carry out perturbation calculations to *all* orders of PT, the λ^2 PT results are more realistic for the Morse potential than the λ^4 PT. The MC method, though numerical in nature, is one way of doing PT to all orders.

We have mentioned in the Introduction that Shukla and Cowley have found that the ISC scheme of selecting diagrams [which represent the total of the (a), (b), (c), and (d) diagrams of Fig. 2] gave good agreement with the MC results for the LJ potential but such a scheme for the Morse potential would yield results not very different from the λ^2 theory. To illustrate reasons for this, we present in Table I the numerical magnitudes for the eight diagrams of $O(\lambda^4)$ presented in Fig. 2. In this table we also present the subtotals for the first two, first four, first six, and the final total for both potentials. These subtotals represent the contributions of the first-order self-consistent (SC1), improved self-consistent (ISC), and second-order self-consistent (SC2) phonon theories of anharmonicity of $O(\lambda^4)$ to the Helmholtz function. The numbers for some diagrams for the LJ potential in Table I differ from Shukla and Wilk because these are more accurately calculated values. It is clear from these results that, whereas for the LJ case, the ISC total is approximately one-half of the total λ^4, $F(\lambda^4)$, the corresponding total for the Morse potential is approximately 17 times smaller than $F(\lambda^4)$. This small correction is not significant enough to change the results of the λ^2 PT. Thus we expect the ISC curve for the Morse potential to be the same as the λ^2 PT which in turn is very close to the MC results. In this sense the Morse and Lennard-Jones MC results are similar.

The MSD results for Xe in the temperature range 60 K $\leq T \leq$ 160 K for the Morse potential are presented in Table II. The MC result refers to 256 particles. The lattice-dynamics (LD) result is the sum total of the quasiharmonic and the λ^2 contribution to MSD which for the sake of comparison with the MC result has been calculated for 256 wave vectors. The zero-pressure lattice parameters, at which these calculations have been carried out, are the MC values (presented in Table II) which are almost the same as the λ^2 PT values. We have also calculated the converged values for the LD case and these are also presented in the last column of Table II, but in the absence of converged MC results we cannot compare them with the corresponding MC values. Once again, we find fairly good agreement between the MC and LD results.

As stated earlier, the λ^2 and λ^4 PT results have been compared with the MC results for all thermodynamic properties for the NNCF model of the fcc lattice with a

TABLE II. Mean-square displacement in units of (Å)^2 for samples with 256 wave vectors or atoms, respectively.

Temperature (K)	Lattice parameter a (Å)	MC (256 particles)	LD (256 wave vectors)	LD (converged)
60	6.1750	0.061 47	0.060 22	0.070 26
80	6.2000	0.086 90	0.085 26	0.099 40
100	6.2275	0.115 15	0.113 84	0.132 61
120	6.2550	0.144 60	0.145 88	0.169 81
140	6.2800	0.176 83	0.180 61	0.210 07
160	6.3100	0.210 98	0.221 62	0.257 55

6-12 LJ interaction potential in Ref. 2. The λ^2 PT results and the MC results for MSD have been compared in Ref. 3. Some other comparisons of the MC results and the λ^2 PT for the Bobetic and Barker potential[16] as well as the Barker, Fisher, and Watts potential[17] for Ar and Kr can be found in Klein and Koehler.[18]

V. CONCLUSIONS

We can draw several conclusions from the thermodynamic and MSD results presented in this paper: (1) The thermodynamic MC results, which include all orders of anharmonicity, are closer to the λ^2 results than the λ^4 PT; (2) Both the MC and λ^2 PT thermodynamic results disagree with the experimental results; (3) for the same sample size (256 particles or wave vectors), the MC and λ^2 PT MSD results agree with each other; (4) a plausible justification of this kind of agreement between the MC and λ^2 PT results for the Morse potential, as given in the text, for a one-dimensional or an isotropic three-dimensional system may be valid in general; (5) based on the small ISC corrections of $O(\lambda^4)$ to F, we conclude that the ISC results for the thermodynamic properties will be essentially similar to the λ^2 PT for the Morse potential and different for the LJ case. In both cases the MC results are close to the ISC results.

ACKNOWLEDGMENT

Two of the authors (R.C.S. and S.K.B.) acknowledge the support of the Natural Sciences and Engineering Research Council of Canada.

[1]R. C. Shukla and F. Shanes, Phys. Rev. B **32**, 2513 (1985).
[2]R. C. Shukla and E. R. Cowley, Phys. Rev. B **31**, 372 (1985).
[3]G. A. Heiser, R. C. Shukla, and E. R. Cowley, Phys. Rev. B **33**, 2158 (1986).
[4]V. Goldman, G. K. Horton, and M. L. Klein, Phys. Rev. Lett. **21**, 1527 (1968).
[5]R. C. Shukla and E. R. Cowley, Phys. Rev. B **3**, 4055 (1971).
[6]R. C. Shukla, Int. J. Thermophys. **1**, 73 (1980).
[7]R. C. Shukla and R. A. MacDonald, High Temp. High Pressures **12**, 291 (1980).
[8]R. C. Shukla and L. Wilk, Phys. Rev. B **10**, 3660 (1974).
[9]R. C. Shukla and C. A. Plint, Phys. Rev. B **40**, 10 337 (1989).
[10]N. Metropolis, A. W. Rosenbluth, M. N. Rosenbluth, A. H. Teller, and E. Teller, J. Chem. Phys. **21**, 1087 (1953).
[11]J. S. Rowlinson, *Liquids and Liquid Mixtures* (Butterworths, London, 1959), p. 266.
[12]P. S. Y. Cheung, Mol. Phys. **33**, 519 (1977).
[13]R. A. MacDonald, R. D. Mountain, and R. C. Shukla, Phys. Rev. B **20**, 4012 (1979).
[14]P. Korpium and E. Lüscher, in *Rare Gas Solids,* edited by M. L. Klein and J. A. Venables (Academic, New York, 1976), Vol. II.
[15]P. M. Morse, Phys. Rev. **34**, 57 (1929).
[16]M. V. Bobetic and J. A. Barker, Phys. Rev. B **2**, 4169 (1970).
[17]J. A. Barker, R. A. Fisher, and R. O. Watts, Mol. Phys. **21**, 657 (1971B).
[18]M. L. Klein and T. R. Koehler, in *Rare Gas Solids,* edited by M. L. Klein and J. A. Venables (Academic, New York, 1976), Vol. I.